**SANDIA REPORT**
SAND2011-8282
Unlimited Release
Printed December 2011

# Including Shielding Effects in Application of the TPCA Method for Detection of Embedded Radiation Sources

Isaac R. Shokair and William C. Johnson

Prepared by
Sandia National Laboratories
Albuquerque, New Mexico 87185 and Livermore, California 94550

Sandia National Laboratories is a multi-program laboratory managed and operated by Sandia Corporation, a wholly owned subsidiary of Lockheed Martin Corporation, for the U.S. Department of Energy's National Nuclear Security Administration under contract DE-AC04-94AL85000.

Approved for public release; further dissemination unlimited.

Sandia National Laboratories

Issued by Sandia National Laboratories, operated for the United States Department of Energy by Sandia Corporation.

**NOTICE:** This report was prepared as an account of work sponsored by an agency of the United States Government. Neither the United States Government, nor any agency thereof, nor any of their employees, nor any of their contractors, subcontractors, or their employees, make any warranty, express or implied, or assume any legal liability or responsibility for the accuracy, completeness, or usefulness of any information, apparatus, product, or process disclosed, or represent that its use would not infringe privately owned rights. Reference herein to any specific commercial product, process, or service by trade name, trademark, manufacturer, or otherwise, does not necessarily constitute or imply its endorsement, recommendation, or favoring by the United States Government, any agency thereof, or any of their contractors or subcontractors. The views and opinions expressed herein do not necessarily state or reflect those of the United States Government, any agency thereof, or any of their contractors.

Printed in the United States of America. This report has been reproduced directly from the best available copy.

Available to DOE and DOE contractors from
U.S. Department of Energy
Office of Scientific and Technical Information
P.O. Box 62
Oak Ridge, TN 37831

Telephone: (865) 576-8401
Facsimile: (865) 576-5728
E-Mail: reports@adonis.osti.gov
Online ordering: http://www.osti.gov/bridge

Available to the public from
U.S. Department of Commerce
National Technical Information Service
5285 Port Royal Rd.
Springfield, VA 22161

Telephone: (800) 553-6847
Facsimile: (703) 605-6900
E-Mail: orders@ntis.fedworld.gov
Online order: http://www.ntis.gov/help/ordermethods.asp?loc=7-4-0#online

SAND2011-8282
Unlimited Release
Printed December 2011

# Including Shielding Effects in Application of the TPCA Method for Detection of Embedded Radiation Sources

Isaac R. Shokair and William C. Johnson

Sandia National Laboratories
Mail Stop 9103
P. O. Box 0969
Livermore, CA 94551-0969

## Abstract

Conventional full spectrum gamma spectroscopic analysis has the objective of quantitative identification of all the radionuclides present in a measurement. For low-energy resolution detectors such as NaI, when photopeaks alone are not sufficient for complete isotopic identification, such analysis requires template spectra for all the radionuclides present in the measurement. When many radionuclides are present it is difficult to make the correct identification and this process often requires many attempts to obtain a statistically valid solution by highly skilled spectroscopists.

A previous report investigated using the targeted principal component analysis method (TPCA) for detection of embedded sources for RPM applications. This method uses spatial/temporal information from multiple spectral measurements to test the hypothesis of the presence of a target spectrum of interest in these measurements without the need to identify all the other radionuclides present. The previous analysis showed that the TPCA method has significant potential for automated detection of target radionuclides of interest, but did not include the effects of shielding. This report complements the previous analysis by including the effects of spectral distortion due to shielding effects for the same problem of detection of embedded sources. Two examples, one with one target radionuclide and the other with two, show that the TPCA method can successfully detect shielded targets in the presence of many other radionuclides. The shielding parameters are determined as part of the optimization process using interpolation of library spectra that are defined on a 2D grid of atomic numbers and areal densities.

## Acknowledgements

Support of this work by the Department of Homeland Security's Domestic Nuclear Detection Office through its Secondary Reachback Program is gratefully acknowledged. The authors would also like to thank Tom Burr, Kristin Hertz, Chris Kunz, and Tim Tooman for useful discussions and comments, and Noel Nachtigal for his support of this work.

# Contents

**1. Introduction** ..... **7**

**2. Incorporation of Shielding Effects in the TPCA Solution** ..... **9**

**3. Generation of Shielded Templates** ..... **11**

**4. Application of TPCA for Detection of Shielded Embedded Sources** ..... **15**

Example with One Target Radionuclide ..... 15
Example with Two Target Radionuclides ..... 19

**5. Effects of Spectral Shape Variation** ..... **23**

Removal of the Background ..... 23
Representation of the Target Spectrum ..... 24

**6. Summary and Conclusions** ..... **27**

**References** ..... **28**

# 1. Introduction

Radiation Portal Monitors (RPMs), have been deployed at border crossings and other locations across the United States for the purpose of detection of illicit radioactive materials, with emphasis on special nuclear materials (SNM). These detectors measure gamma and neutron radiation as a vehicle passes through the portal, producing a series of spectral measurements for each vehicle. The RPM system alarms if a vehicle's profile exceeds a fraction of the background level and/or the energy spectrum has specific characteristics associated with SNM. Vehicles that result in alarms are usually routed for a more rigorous secondary inspection that includes additional spectral measurements as well as imaging of the cargo in some cases.

The measured profiles for the majority of vehicles indicate the absence of radioactivity and show suppression of the ambient background as a result of shadow shielding environmental gamma rays by surveyed vehicle structure and cargo. In a small fraction (~5%) of vehicles, the measured profiles show the presence of radioactive sources that mostly consist of naturally occurring radioactive materials (NORM), but also include other sources such as medical and industrial isotopes. Given the large volume of commerce, the total number of vehicles with radioactive material becomes significant. Since identification of the radiation source through manual inspection of the cargo is time consuming and manpower exhaustive, it is desirable to develop enhanced algorithms and analysis methods that improve the power of detecting illicit sources while reducing the false positive rate (i.e. the ability to distinguish benign and illicit sources of radiation with high confidence). The use of such algorithms in deployed systems would allow for reduction of alarm thresholds to increase sensitivity while improving throughput. The latter is accomplished by the ability to confidently detect and identify cargo with benign sources of radiation at the primary lane without the need to send a vehicle to secondary inspection. Previous studies have explored and demonstrated data transformation methods to differentiate NORM cargo from other nuclides[1-2].

With automated analysis algorithms, it is equally important to consider all realistic scenarios that could result in incorrect conclusions. This is especially important for extremely low probability events that can have major catastrophic consequences, such as terrorist related activity. One such scenario is that of transport of illicit radioactive materials embedded in NORM cargo in an attempt to conceal their radiation signal. A previous study of this type of scenario was conducted for low resolution polyvinyl toluene (PVT) detectors with only two energy channels[3]. This study used the spatial profile of total counts to detect potential embedded sources and then used the available spectral information to determine if the region containing the potential source has statistically significant spectral differences from the remainder of the profile.

A more recent study explored using data fusion of spectral and spatial information to test the hypothesis of presence of a target of interest in a series of measurements using a NaI detector[4]. This study developed a new spectral detection method, referred to as Targeted Principal Component Analysis (TPCA), and tested it for automated detection of embedded sources for RPM applications. This method tests the hypothesis of the presence of one or more target radionuclides of interest without regard to identification of other radionuclides that are present in the measurement by exploiting the spatial/temporal information along with the spectral information. The requirement for this method to work is that the spatial profile for the target

radionuclide(s) of interest is different from other radionuclides present in the measurements. The degree of difference or contrast between the profiles along with analysis parameters will determine the target detection limits. It was shown that the TPCA method is based on sound principles for problems with multiple measurements that encompass the required spatial/temporal variations. One of the limitations of the previous study is that it did not include the effect of spectral distortions due to shielding. This is the subject of this report.

In addition to overall reduction in gamma counts, shielding results in spectral distortions due to energy dependent attenuation and Compton scattering. For a given detector response, these distortions can be described by nonlinear parametric models or by interpolation between known spectra at different shielding parameters. In this report we use a simple interpolation method to model shielded target spectra for a specific detector at any set of atomic number and areal density of a shielding material. The TPCA method is applied as in the previous report, except that the target spectrum or spectra are no longer constant, but are functions of the shielding atomic number (AN) and areal density (AD). The optimal AN and AD are found using a nonlinear optimization algorithm.

In section 2 of the report the TPCA method is outlined for target spectra that include unknown shielding. This section also describes implementation of the method and the nonlinear optimization algorithm used to estimate the shielding parameters. In section 3 the interpolation method for obtaining shielded target spectra at any set of shielding parameters is described. This interpolation uses a library of shielded spectra that is generated using GADRAS 1D models[5-6]. Section 4 of the report shows results for two test cases, one with a single target radionuclide and the other with two. The results validate the method for shielded targets within the limits of the assumptions made for the simulations. Section 5 discusses the effects of target and background spectral variation as a function of space and the limits imposed by these variations on detection capability. The last section of the report summarizes the results.

The results presented here and in reference (4) validate the use of the TPCA method for detection of embedded sources and other applications where spatial/temporal variation between the target of interest and other clutter is present. Much research is needed however to understand the sensitivity of results on the chosen analysis parameters and to optimize these parameters for optimal detection limits.

## 2. Incorporation of Shielding Effects in the TPCA Solution

As discussed in reference (4), the target spectrum of interest can be expressed as a linear combination of principal component (PC) spectra derived from all or a subset of the measurements under considerations as:

$$T(E, AN, AD) \approx \sum_{i=1}^{N'} \alpha_i \; P_i(E) \qquad N' << N \tag{1}$$

where $P_i(E)$ denotes the i$^{th}$ PC spectrum and $N'$ is the number of PC spectra to be used in the analysis, which is assumed to be much smaller than the number of available measurements when the number of measurements is large. If the number of measurements is small, they can be used directly instead of the PC spectra. The target spectrum including shielding effects is now a function of the atomic number, *AN*, and areal density, *AD*, which are not known and will be treated as optimization parameters in the solution process. As before, the quantity to be minimized for testing the target hypothesis is the reduced residual $\chi^2$ given by:

$$\chi^2 = \frac{1}{(M_c - N')} \sum_{j=1}^{M_c} \frac{\left[ T(E_j, AN, AD) - \sum_{i=1}^{N'} \alpha_i \; P_i(E_j) \right]^2}{\hat{\sigma}^2(E_j)} \tag{2}$$

where $M_c$ is the number of energy channels and $\hat{\sigma}^2(E_j)$ is the estimated statistical variance of the calculated fit of the target spectrum for the j$^{th}$ energy channel. This variance is due to statistical measurement noise and needs to be distinguished from physical variance between measurements at different time samples as varying combinations of the various sources are sampled by the detector as the vehicle traverses the RPM. Note that $(M_c - N')$ is the number of degrees of freedom. When the target of interest is made 2up of multiple radionuclides such as for uranium or plutonium, the target spectrum is replaced by a linear combination of the individual spectra of the radionuclides that make up the target and the reduced residual becomes:

$$\chi^2 = \frac{1}{\left(M_c - N' - [\nu - 1]\right)} \sum_{j=1}^{M_c} \frac{\left[ \sum_{i=1}^{\nu} \beta_i \; T_i(E_j, AN, AD) - \sum_{i=1}^{N'} \alpha_i \; P_i(E_j) \right]^2}{\hat{\sigma}^2(E_j)} \tag{3}$$

where ν is the number of radionuclides in the target; $T_i(E_j, AN, AD)$ represent the shielded spectra for the individual target radionuclides (all target radionuclides are assumed to have the same shielding parameters for analysis considered in this report); and the coefficients, $\beta_i$, denote the unknown relative isotopic composition. One of these coefficients is arbitrary and can be set to unity and therefore the number of degrees of freedom is reduced by (ν - 1). The objective of the analysis is to calculate the coefficients and shielding parameters that minimize the $\chi^2$ residual as given by equation (3) to evaluate the statistical plausibility of the assumed target hypothesis.

The variance is estimated based on expressing the PC spectra as linear combinations of the measurements and as discussed in the previous report (see reference 4) is given by:

$$\hat{\sigma}^2(E) \approx \sum_{k=1}^{N} (\mu_k)^2 \text{ variance } [M_k(E)] \tag{4}$$

$$\mu_k = \sum_{i=1}^{N'} \frac{\alpha_i}{\lambda_i} (M_k \bullet P_i) \tag{5}$$

where $\alpha_i$ is the coefficient associated with the i$^{th}$ PC vector $P_i$ in equation (3); $\lambda_i$ is the eigenvalue associated with the same PC vector; and $M_k$ denotes the k$^{th}$ measurement vector. The variance of the k$^{th}$ measurement is estimated as the filtered measured spectrum based on the assumption of Poisson statistics for the counts in a spectral channel. Since the variance depends on the calculated optimization parameters and coefficients, an iterative method is used where the current variance is estimated based on the calculated parameters and coefficients for the previous iteration. For the first iteration a constant unit variance is assumed. For the test cases considered, convergence of the variance typically occurs within two or three iterations.

As discussed in the previous section, the shielded target spectrum depends on the shielding parameters *AN* and *AD* in a nonlinear manner for a given detector. These parameters are estimated using a hybrid linear-nonlinear optimization method. In the current implementation of this method, the nonlinear optimization is performed using Powell's method as implemented in the Numerical Recipes function POWELL[7]. This function calls a wrapper function of only two variables (the nonlinear parameters *AN* and *AD*) which in turn calls a C++ function (residual function) that is a member of a class with access to all the needed data (the wrapper function uses a pointer to this class object). This function evaluates the needed target spectra for the given shielding parameters and uses linear least squares (LS) optimization to evaluate all the linear coefficients in equation (3) and the resulting residual. This residual is passed back to POWELL which repeats the process for other sets of the shielding parameters until convergence is attained. This process is repeated for all variance estimate iterations.

To avoid convergence to a possible local minimum we implemented a modification to the above method where the residual function is evaluated on a coarse 2-D grid of *AN* and *AD* values. The minimizing *AN* and *AD* are used as initialization to the function POWELL. This method appears to work very well and is reasonably fast. For the present implementation a 10x10 grid is used.

In the current implementation and for multiple radionuclides, the first target coefficient, $\beta_1$, is set to unity and the remaining coefficients are evaluated in the LS process along with the PC coefficients. This can be problematic if target spectra associated with the remaining coefficients do not possess an orthogonal component to the PC spectra. In such a situation the LS coefficient matrix will be singular and an erroneous solution will result. In general, we think it is best to separate evaluation of the PC coefficients from the target coefficients. This should also allow for imposing the constraint that all target coefficients are positive quantities. An algorithm that separates calculation of the two sets of coefficients can be considered in the future.

## 3. Generation of Shielded Templates

In order to automate the process of generating and fitting the shielded templates in this study, a library and interpolation scheme was created in order to produce templates corresponding to a given nuclide and shielding configuration in the analysis software; henceforth this library and interpolation scheme will be referred to as the template library. For the nuclides considered in this study ($^{137}$Cs, $^{235}$U, and $^{238}$U) the template library can produce a shielded template with an arbitrary Areal Density (AD) and Atomic Number (AN) within some ranges. The template library works by interpolating between basic templates generated using GADRAS[5-6] to produce a new template corresponding to the AD and AN desired by the analysis software. To begin with, GADRAS was used to create spectra for each of the nuclides with 8 atomic numbers between 7 and 50, and 11 areal densities between 0 to 100 g/cm$^2$ [a], yielding a total of 88 templates per nuclide. The shielding configuration was modeled within GADRAS as a uniform 1D spherical model with 1 meter radius, made of the element corresponding to the AN and the density to the AD of the template being produced. The default GR-135 detector (handheld NaI detector) that comes with GADRAS was used as the detector model, with no sources of radiation besides the nuclide desired being present in the simulation.

In order to use a non-linear optimization algorithm to fit a spectrum for the most probable shielding and nuclide configuration, one must be able to obtain templates which can be continuously varied in AD and AN. To accomplish this, an interpolation scheme was used to interpolate between the discreet numbers of templates produced using GADRAS. It was found that for a given energy bin in the spectrum, the amplitude varies approximately linearly in AN, and exponentially in AD[b]. That is to say, for the i$^{th}$ bin in the spectrum, to obtain the expected bin height $b_i$, for a AN of $Z$, using input templates with ANs of $Z_1$ and $Z_2$ (which have identical ADs), and bin contents $b_{i,1}$ and $b_{i,2}$, the following formula was used:

$$b_i(Z) = b_{i,1} + \frac{Z - Z_1}{Z_2 - Z_1}\left(b_{i,2} - b_{i,1}\right) \tag{6}$$

For the exponential interpolation to obtain a template for a given AD, the bin contents were found using

$$b_i(AD) = b_{i,1}\left(\frac{b_{i,2}}{b_{i,1}}\right)^{(AD-AD_1)/(AD_2-AD_1)} \tag{7}$$

where AD denotes the desired areal density, $b_{i,1}$ and $b_{i,2}$ corresponding to the bin contents of the spectra with areal densities $AD_1$ and $AD_2$ respectively; both templates with $AD_1$ and $AD_2$ have

[a] The actual values of ANs used are 7, 11, 15, 20, 25, 31, 40, and 50. The actual values of ADs used are 0, 5, 10, 15, 20, 25, 30, 40, 50, 70, and 100 g/cm$^2$.

[b] For the photopeaks themselves, the amplitude is actually exponentially dependent on the AD; for gammas detected at a given energy originating from a photopeak of a different energy, which have undergone scattering, pair-production, or the photo-electric effect, this approximation holds true over reasonable ranges of AN.

the same atomic numbers. The templates chosen to interpolate from are the four templates nearest in AD and AN to the desired template (the input templates from GADRAS are generated on a grid of AN and AD values); the templates are first interpolated in AD, producing two new templates corresponding to the same AD, but different ANs. These two intermediate templates are then interpolated in AN to achieve the final template.

Some example results of this interpolation are shown in Figures 1-2 where it can be seen the resulting interpolated spectra agree well with that produced directly from GADRAS.

In order to determine limits of this interpolation method, as well as identify the mechanisms behind the *slight* inaccuracies, a study was performed using the Monte Carlo simulator GEANT4 where individual photons were tracked and classified according to what interactions were undergone. The interpolation was then performed on templates consisting solely of gammas that interacted in similar ways in the shielding (e.g. single scatter events were grouped into one template, multiple scatter into another, non-interacting gammas into another, and so on). The results and comparison of direct simulations to interpolating the individual physics processes from ADs of 25 and 50 g/cm$^2$ to get 35 g/cm$^2$ is shown in Figure 3 and performs fairly well. Figure 4 shows a similar comparison, but for interpolating from AN 18 and 33 to get AN 23; as expected gammas which go through multiple scattering do not interpolate well, and are responsible for the majority of the inaccuracies from this interpolation scheme. The actual differences of AD and AN of templates used to interpolate from in the following TPCA analysis are much smaller than in Figures 3-4 (see footnote a).

Overall the inaccuracies introduced by using this library/interpolation are smaller than many other real world effects, so this method of producing templates to model sources and fit to simulated spectra is suitable for this limited study.

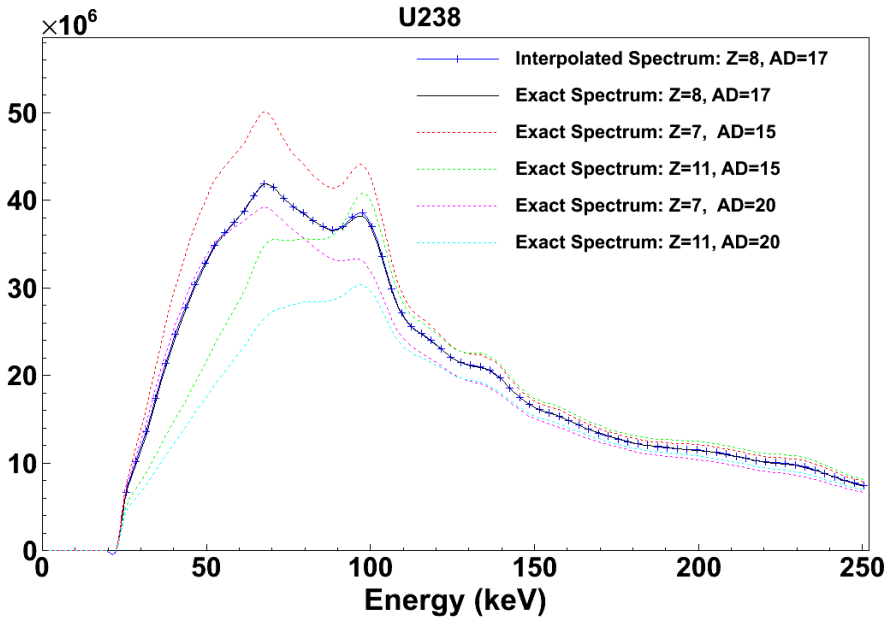


**Figure 1**. Interpolation of a $^{238}$U spectrum to a AN of 8, and AD of 17. The blue line (mostly hidden by the black line) with small crosses in each bin is the result of the interpolation, while the solid black line is directly produced using GADRAS (and not used in the interpolation process); the four spectra with dashed lines were used to interpolate to the final (blue) template. The interpolated spectrum is almost identical to the one directly calculated by GADRAS.

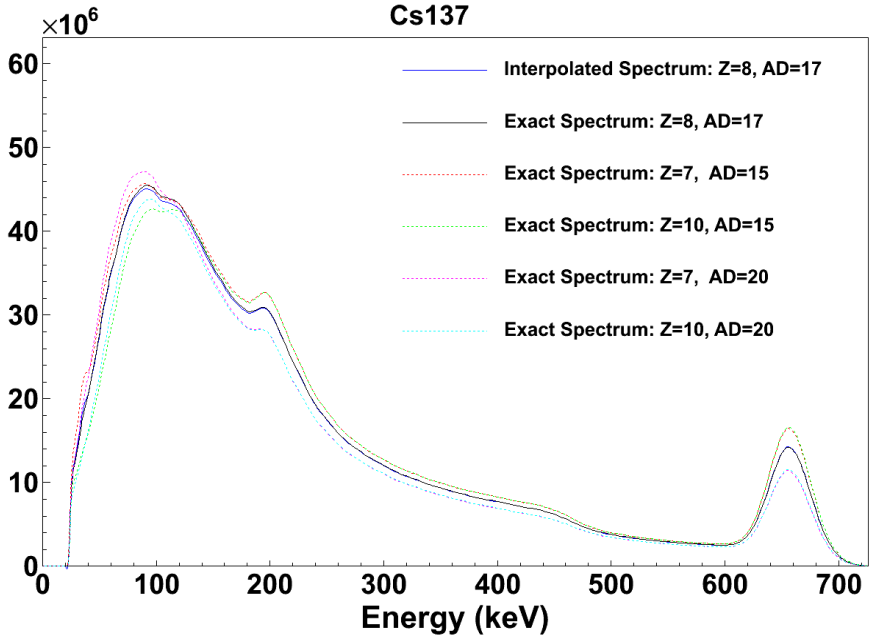


**Figure 2**. A comparison of the interpolated $^{137}$Cs spectrum (blue solid line) corresponding to AN 8, and AD 17, to the spectrum produced by GADRAS (black solid line) corresponding to the same AN and AD. The four templates used to produce the interpolated spectrum are also shown in the dotted lines.

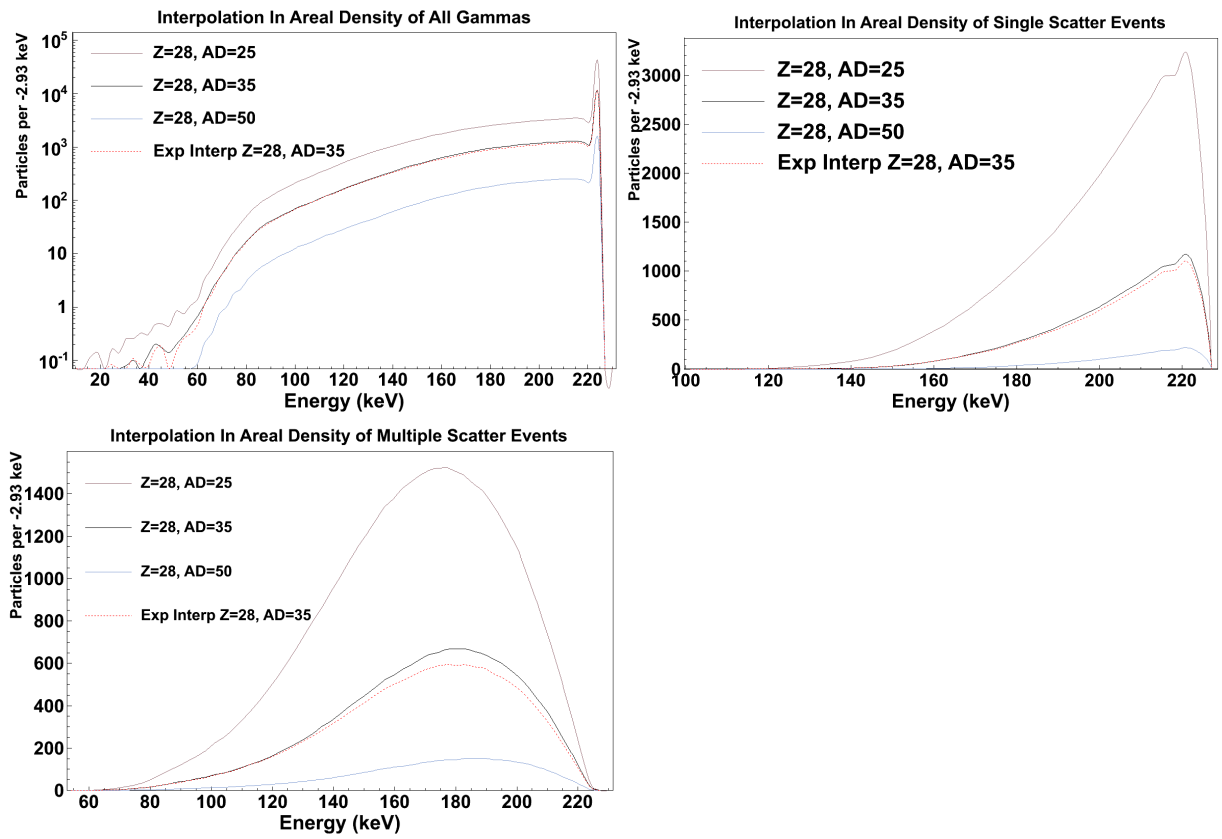


**Figure 3.** A comparison of interpolation in AD of 225 keV gammas shielded by a material with AN=28, and areal densities 25, 35, and 50 g/cm$^2$; the 25 and 50 g/cm$^2$ templates were interpolated to compare to the 35 g/cm$^2$ template. The templates were generated using GEANT4 and no detector response. The upper left plot shows the spectra where all gammas exiting the shielding are included. The upper right plot show gammas exiting the shielding that underwent one scattering event. The lower plot shows event where the gammas underwent at least 2 scattering events.

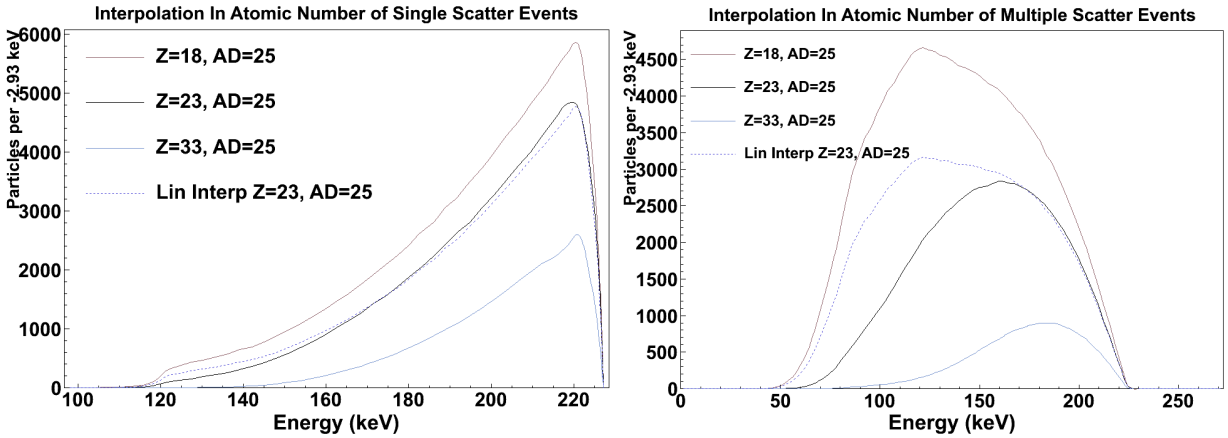


**Figure 4**. Interpolation in AN between AN 18 and 33, to get a template of AN 23; all templates had an AD of 25 g/cm$^2$; the result of this interpolation is compared to the non-interpolated template of AN 23. The templates were produced using GEANT4 with no detector response. The left plot contains only single scatter events, while the right contains events with at least 2 scatters. It is seen that interpolating in AN for single scatter events is accurate, while interpolating multiple scatter events does not perform so well.

# 4. Application of TPCA for Detection of Shielded Embedded Sources

In this section we present simple examples of the application of the TPCA method for detection of a localized shielded source that is embedded in a distributed source in the presence of an ambient background using the algorithm outlined in the previous section. This is done in the context of an RPM measurement of a vehicle with multiple spectral measurements at contiguous time samples as the vehicle traverses the RPM. The combinations of radionuclides used for the sources and background were chosen to generate sufficiently complex spectra for illustrative purposes only, and do not reflect any specific real measurement. The effect of background suppression is not included in this analysis, but is not expected to result in significant adverse effects in application of the TPCA method even if it is large.

Before discussing actual examples, we summarize the assumptions made for generation of the simulation spectra:

1. All counts follow Poisson statistics. This assumption does not impact effectiveness of the TPCA method. If the measurements or simulations follow other statistics, the only requirement is that the correct variance, corresponding to the counting statistics, is used in equation (4).

2. The target spatial profile is modeled by a point source profile and the other sources are modeled by a constant ambient background and a distributed source profile. This is not a requirement for application of the TPCA method. The spatial variation required for correct application of this method is that the spatial profiles for the target and the other sources are sufficiently different to allow for removal of the background without singular behavior. Of course larger differences in the spatial profiles will result in better detection sensitivity.

3. The net spectrum at every point along the profile is a linear superposition of the different source spectra. The source spectra are assumed constant for the analysis in this section. This assumption is not strictly required by TPCA, but spectral variation adds complexity to the solution. Also, depending on the spatial profiles, spectral variation can add uncertainty to the solution results. This topic will be discussed further in section 5 of this report.

## Example with One Target Radionuclide

For this test the localized source is a shielded $^{137}$Cs source that is embedded in a distributed source and a spatially uniform background. The shielded localized source spectrum is obtained using the template library described in the previous section at shielding parameters AN of 17.75 and AD of 25.0 g/cm$^2$. The distributed source is made up of a mixture of four isotopes ($^{226}$Ra, $^{232}$U, $^{201}$Tl, and $^{60}$Co). The background spectrum is made up of two isotopes ($^{40}$K and $^{232}$Th). The spectra for the distributed source and background as well as the spatial distributions for all sources are identical to those used in our previous report[(4)]. The model spectra are shown in Figure 5. Scaling of the counts in generation of simulation spectra will be directly applied to the spectra shown in this figure.

The spatial distributions for the localized and distributed sources used in the analysis are shown in Figure 6 and are given by:

$$f_P(z) = A_P \left[ \frac{R_0^2}{R_0^2 + (z - z_o)^2} \right]^{3/2} \tag{8}$$

$$f_D(z) = \alpha_0 \left\{ \frac{z - z_o + \Delta}{\left[ R_o{}^2 + (z - z_o + \Delta)^2 \right]^{1/2}} - \frac{z - z_o - \Delta}{\left[ R_o{}^2 + (z - z_o - \Delta)^2 \right]^{1/2}} \right\} \tag{9}$$

$$f_D(z = z_0) = \frac{2\,\alpha_0\,\Delta}{\left[ R_0^2 + \Delta^2 \right]^{1/2}} \equiv A_D \tag{10}$$

where $P$ denotes the point or localized source, $D$ denotes the distributed source, and $(z - z_0)$ is the distance from the source center to the center of the detector along the direction of vehicle motion. The source amplitudes are denoted by $A_p$ and $A_D$, $R_0$ is a measure of the perpendicular distance from source to detector, and $\Delta$ denotes the half-width of the distributed source. The source parameters are formally defined in appendix B of reference (4). The simulated measured spectrum as a function of time sample (or position along direction of vehicle motion) is given by the profile-modulated model spectra as follows:

$$S(z, E) = C_p\, S_P(E)\; f_P(z) + C_D\, S_D(E)\; f_D(z) + C_B\, S_B(E) \tag{11}$$

where the profile modulation functions $f_P(z)$ and $f_D(z)$ are given by equations (8) and (9). The spectra $S_P(E)$, $S_D(E)$, and $S_B(E)$ are the point source, distributed source, and background spectra respectively that are shown in Figure 5 above. The coefficients $C_P$, $C_D$, and $C_B$ are used to scale the counts given in this figure. Poisson statistics are applied to the simulation spectra as given by equation (11) at all $z$ and $E$ values.

The test case considered has scale factors: $C_P = 0.2$, $C_D = 0.2$, and $C_B = 0.2$ and a total of 160 time samples are used. The simulated spectra represent measurements at different time samples as the vehicle passes through the portal. The number of spectral channels is reduced from 1024 to 256 in the analysis. A total of 100 statistical repetitions of spectral generation and TPCA solution were carried out to estimate the spread in analysis output quantities. The total counts profile and spectrum at maximum counts are shown in Figure 7 for the first statistical set. Figure 8 shows the detection analysis results for the same statistical set. Table 1 shows the spread of the solution parameters for the 100 statistical repetitions. For all these repetitions the resulting fit to the target spectrum is very good and clearly indicates the presence of the target in the simulated measurements.

Even though the signal to noise ratio is rather high, this example illustrates that the TPCA method is capable of handling spectral distortion due to shielding and allows for target detection without using any knowledge concerning the other clutter radionuclides. Further analysis is needed to study methods of optimization of detection limits.

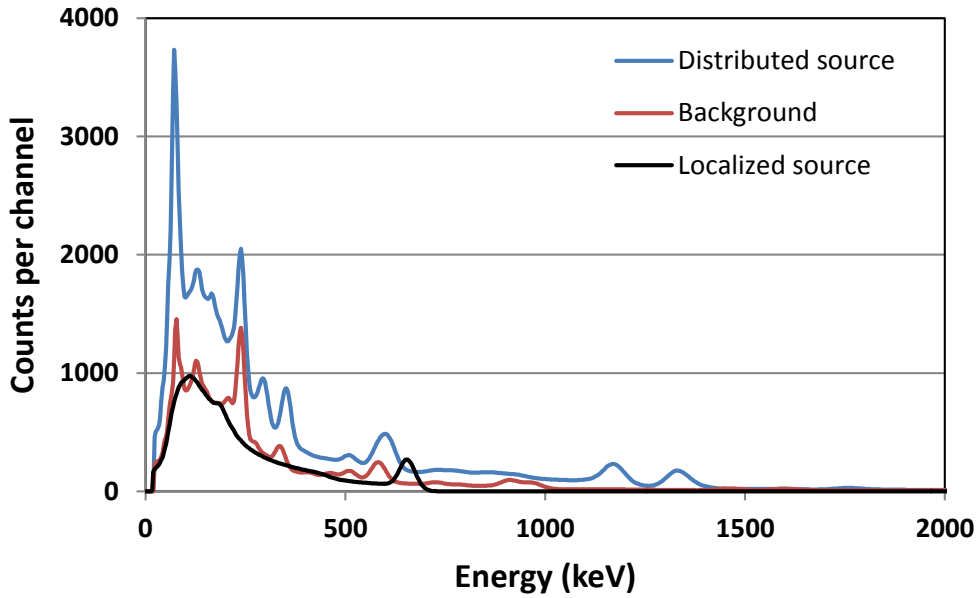


**Figure 5**. Model spectra for the sources and background. The distributed source spectrum is the sum over GADRAS model spectra for $^{226}$Ra, $^{232}$U, $^{201}$Tl, and $^{60}$Co, each at 10 μCi for a GR-135 detector at 100 cm distance. The background is the sum over model spectra for $^{40}$K and $^{232}$Th, each at 10 μCi for the same detector parameters. The localized source is shielded $^{137}$Cs (atomic number 17.75 and areal density 25.0 g/cm$^2$) obtained from the template library (scaled by 30,000 for a comparable amplitude to the other sources). The model spectra have 1024 channels in the range 0 to 3653.0 keV.

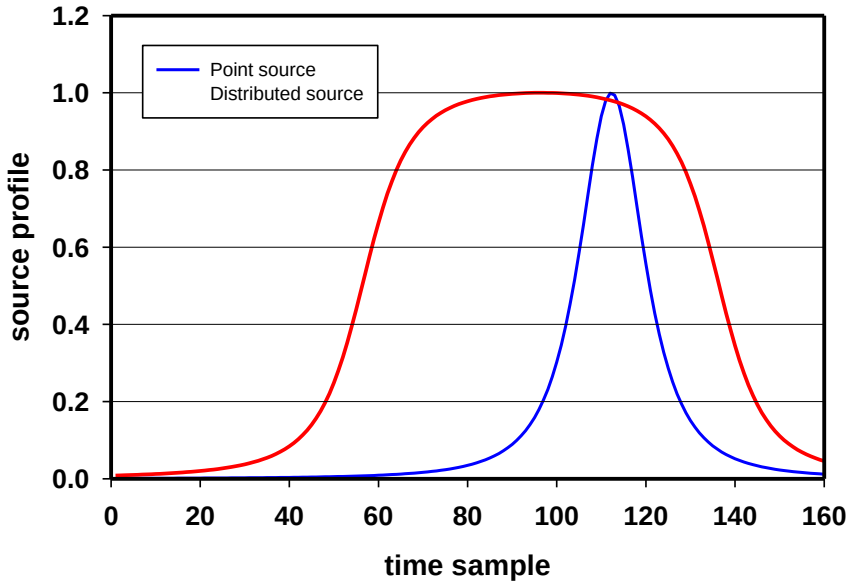


**Figure 6**. Model profiles for point and distributed sources. All spatial quantities are normalized to the overall vehicle length and the first and last time samples correspond to the entry and exit of the vehicle from the portal respectively. A total of 160 time samples are used. The normalized source parameters are: Point source: $z_o = 0.7$, $R_o = 0.07$. Distributed source: $z_o = 0.6$, $R_o = 0.07$, $\Delta = 0.25$.

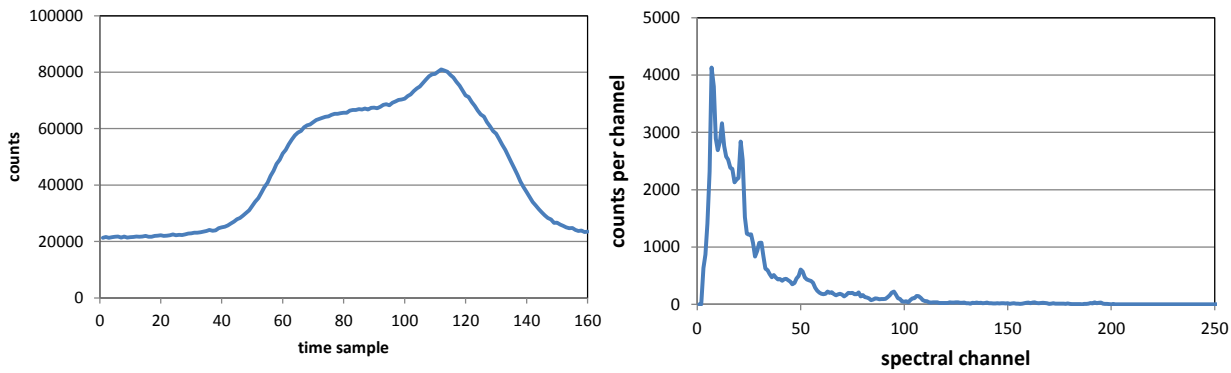


**Figure 7**. Left: total counts profile as a function of time sample. The sources and background spectra are scaled from the model spectra in Figure 5 by the factors: $C_P = C_D = C_B = 0.2$. The source geometric parameters are the same as in Figure 6. Right: simulated spectrum at time sample of maximum counts. The number of spectral channels is reduced from 1024 to 256.

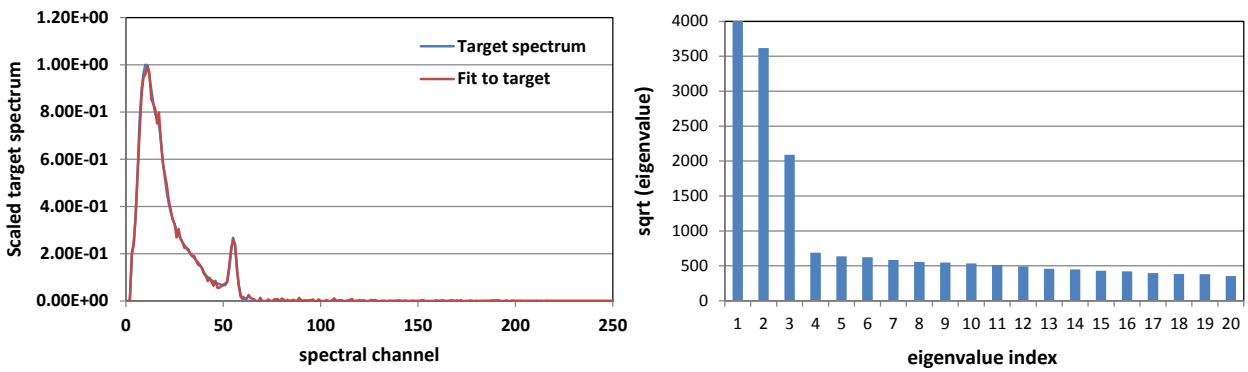


**Figure 8**. Left: shielded target spectrum and fit using 5 PC spectra for source scale factors of $C_P = C_D = C_B = 0.2$. The number of energy channels is reduced from 1024 to 256 in the analysis. The residual for this simulation is $\chi^2 = 1.11$. Right: the first 20 eigenvalues in descending order for the PC spectra. The first eigenvalue represents the mean of all the measurements used in obtaining the PC spectral vectors and is very large (off scale). The next two eigenvalues represent most of the remaining variance due to spectral differences between the localized source, distributed source, and background. The other eigenvalues mostly represent noise contributions. If Poisson noise is turned off in the simulations only three eigenvalues are non-zero and the fit to the target spectrum using the three corresponding eigenvectors is perfect. Note that in the PCA the covariance matrix is evaluated about the origin rather than the mean spectrum.

**Table 1**. Spread in solution parameters for 100 statistical sets for detection of a shielded $^{137}$Cs localized target embedded in a distributed source and a uniform background. The input target spectrum had shielding parameters of AN 17.75 and AD 25.0 g/cm$^2$.

| Solution parameter | Mean | Standard Deviation | Minimum | Maximum |
|---|---|---|---|---|
| $\chi^2$ | 1.074 | 0.095 | 0.85 | 1.34 |
| Atomic number | 17.2 | 0.54 | 15.9 | 18.9 |
| Areal density | 25.4 | 0.81 | 22.2 | 28.6 |

## Example with Two Target Radionuclides

In this section a more complex example with two target radionuclides is considered for the localized source. The target radionuclides are $^{235}U$ and $^{238}U$ including their daughter products. The distributed source and background are identical to the previous example. The input localized source spectrum for the simulations is obtained from the template library at shielding parameters of AN 13.0 and AD 20 g/cm$^2$ and is made up of a ratio of 1:1.3 of $^{238}U$ to $^{235}U$ relative to the template library. The source spectra are shown in Figure 9.

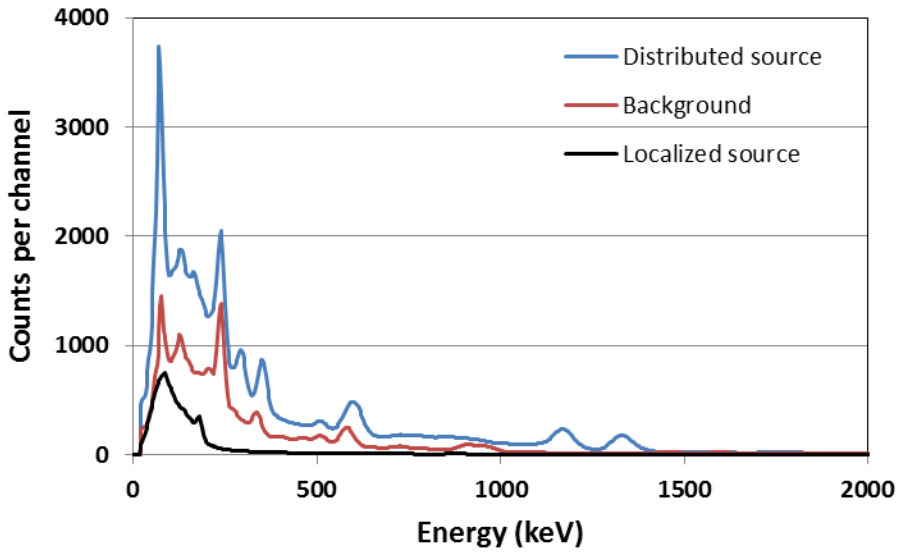


**Figure 9**. Model spectra for the sources and background. The distributed source and background spectra are identical to those in Figure 5. The localized source spectrum is for shielded uranium (shielding parameters: AN 13.0 and AD 20.0 g/cm$^2$) for a 1:1.3 ratio of $^{238}U$ to $^{235}U$ based on the template library spectra.

The test considered has scale factors: $C_P = 0.4$, $C_D = 0.1$, and $C_B = 0.1$ and a total of 160 time samples are used. The number of spectral channels is reduced from 1024 to 256 in the analysis. Two independent target radionuclides were considered in the analysis ($^{238}U$ and $^{235}U$) with the same unknown shielding parameters. The ratio of $^{238}U$ to $^{235}U$ as represented by the coefficient $\beta$ in equation (3) is one of the unknowns and was solved for in the same linear LS optimization process along with the PC coefficients $\alpha$. This method was used for ease of implementation, but is not the ideal method and can lead to singular behavior as alluded to earlier in this report. Other solution methods can be considered in the future.

A total of 100 statistical sets were repeated to quantify spread in solution parameters. The total counts profile and spectrum at maximum counts are shown in Figure 10 for the first statistical set. Figure 11 shows the detection analysis results for the same statistical set and the table below shows the spread of the solution parameters for the 100 repetitions. Even though the estimated shielding parameters are very close to the input values, the $^{238}U$ to $^{235}U$ ratio is significantly different from the input value. This will require further investigation to understand and quantify. However, we should note that a test run at significantly higher target SNR (scale factors of $C_P$ =

4.0, $C_D$ = 0.1, and $C_B$ = 0.1) resulted in an average ratio of 0.76 with a standard deviation of 0.013 which is much closer to the input value. Thus the discrepancy appears to be related to the SNR, but one would have expected a larger spread in values rather than an offset in the mean. This needs to be further investigated.

For the same parameters used in this example we tested a different target hypothesis, namely shielded $^{137}$Cs. The results of one statistical set are shown in Figure 12 and the spread in estimated parameters is shown in table 3 below. Clearly for this case one can conclude that $^{137}$Cs is not the correct target hypothesis.

**Table 2**. Spread in solution parameters for 100 statistical sets for detection of a shielded $^{238}$U + $^{235}$U localized target embedded in a distributed source and a uniform background.

| Solution parameter | Mean | Standard Deviation | Minimum | Maximum |
|---|---|---|---|---|
| $\chi^2$ | 1.08 | 0.128 | 0.80 | 1.46 |
| Atomic number | 13.1 | 0.068 | 12.9 | 13.2 |
| Areal density | 21.8 | 0.93 | 18.6 | 22.2 |
| Ratio of $^{238}$U to $^{235}$U | 0.51 | 0.061 | 0.37 | 0.65 |

**Table 3**. Spread in solution parameters for 100 statistical sets for detection of a shielded $^{238}$U + $^{235}$U localized target embedded in a distributed source and a uniform background. The target hypothesis is assumed to be $^{137}$Cs

| Solution parameter | Mean | Standard Deviation | Minimum | Maximum |
|---|---|---|---|---|
| $\chi^2$ | 19.1 | 2.65 | 12.3 | 23.3 |
| Atomic number | 11.0 | 0.1 | 11.0 | 11.8 |
| Areal density | 88.9 | 2.53 | 80.1 | 100.0 |

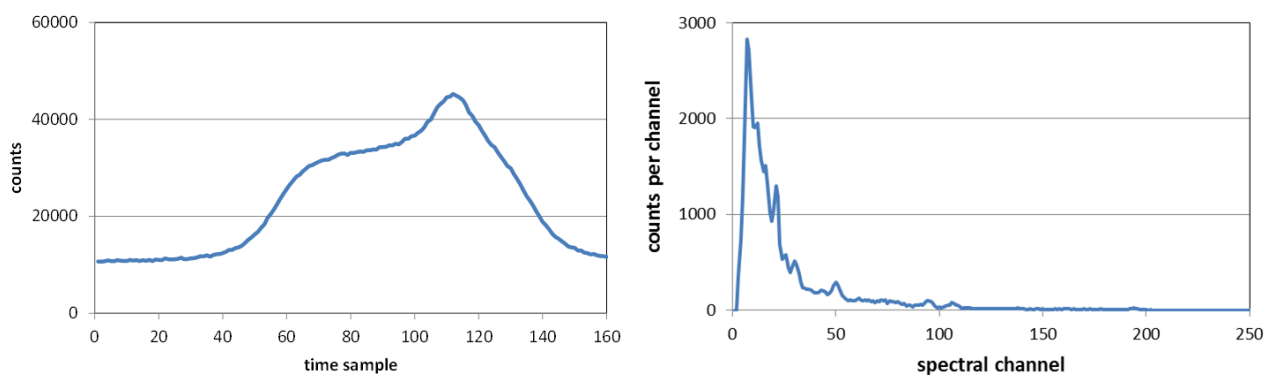


**Figure 10**. Left: total counts profile as a function of time sample. The sources and background spectra are scaled from the model spectra in Figure 9 by the factors $C_P$ = 0.4 and $C_D$ = $C_B$ = 0.1. Right: simulated spectrum at time sample of maximum counts. The number of spectral channels is reduced from 1024 to 256 for this test.

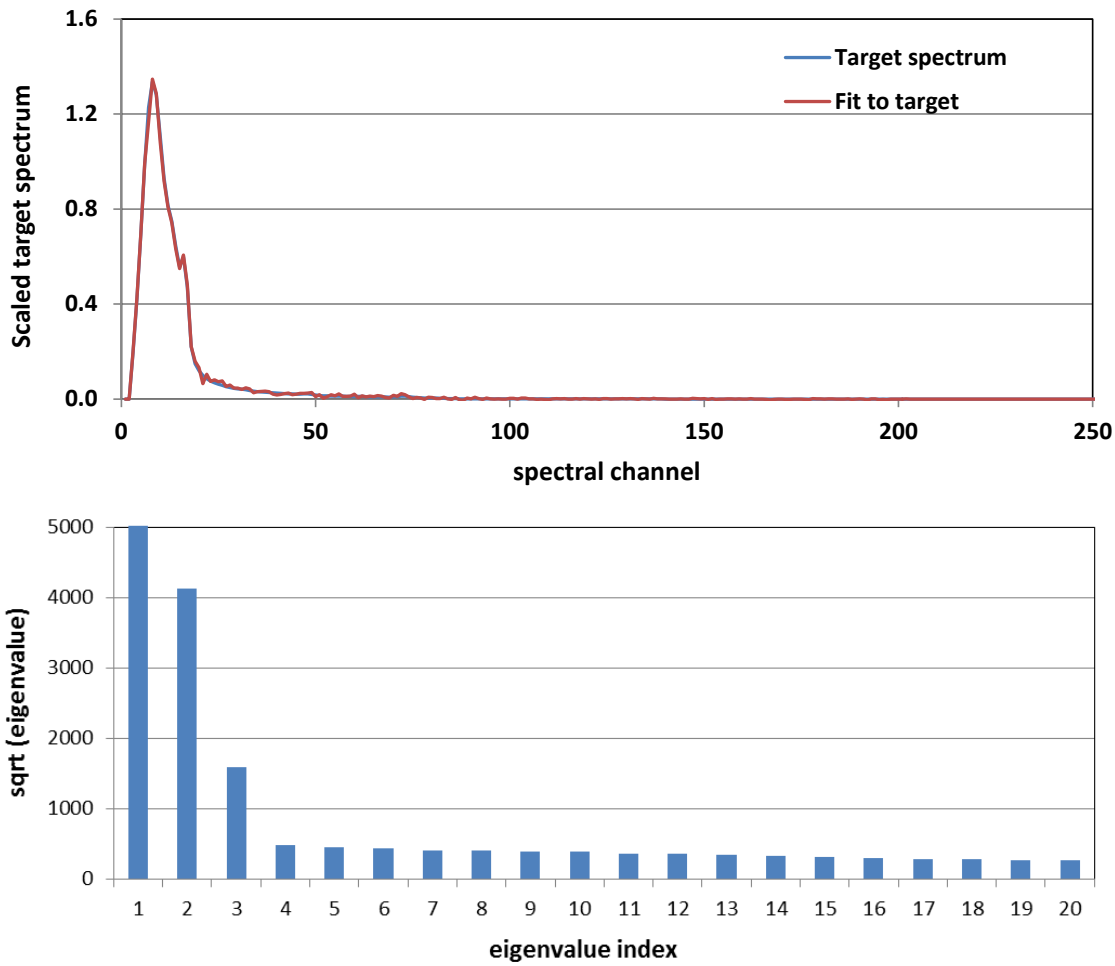


**Figure 11**. Top: shielded target spectrum and fit using 5 PC spectra. The target spectrum is made up of a linear combination of shielded $^{238}$U and $^{235}$U spectra. The shielding parameters (same for the two isotopes) and isotopic ratio are unknown parameters that are estimated in the optimization process. The number of energy channels is reduced from 1024 to 256 in the analysis. The residual for this simulation is $\chi^2$ = 1.06. Bottom: the first 20 eigenvalues in descending order for the PC spectra. The first eigenvalue represents the mean of all the measurements used in obtaining the PC spectral vectors and is very large (off scale).

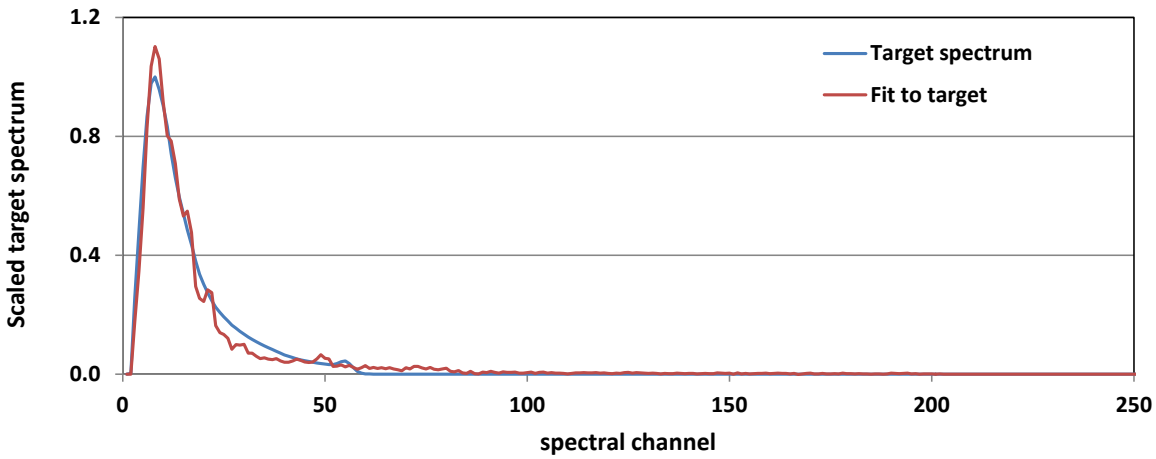


**Figure 12**. Shielded target spectrum and fit using 5 PC spectra with $^{137}$Cs as the hypothesis target. The simulation parameters are identical to those in Figure 11. For this case the $\chi^2$ residual is 17.2 and the shielding parameters are AN = 11.0 and AD = 88.9. The large $\chi^2$ indicates that the hypothesis target isotope is not correct.

# 5. Effects of Spectral Shape Variation

In the example simulations considered in the previous section, the amplitudes of the localized and distributed sources were varied as a function of time, but the shielding composition (areal density and atomic number), and hence the spectral shape, remained constant. For real world measurements the shielding configuration can change as the distance and angle between source and detector change. Additionally, the ambient background undergoes varying suppression as the vehicle structure and cargo move past the detector. Along with the change in suppression amplitude it is possible that the background spectral shape will also change.

An important concern is how this spectral variation affects the application and results of the TPCA method. This method relies on removing the background (meaning all non-target sources) which is done automatically in the process of testing the target-presence hypothesis (see section 2 of reference 4). This means that a linear combination of the measurements, capable of removing the background, needs to exist. In addition, this linear combination needs to be representable by a model of the target spectrum. This model can be one or more spectra for each of the target radionuclides at some effective shielding parameters. In this report we limit the target hypothesis to one spectrum per constituent radionuclide and will show later in this section that this is a reasonable approximation for the embedded sources problem. More complex target models can be considered in future work.

## Removal of the Background

As discussed earlier, the TPCA method automatically removes the background. When the background spectral shape is constant for all the measurements, this process is simple and only requires different spatial profiles for the target and background. If both target and background have identical spatial profiles, removing the background would also remove the target resulting in singular behavior.

With variation of the background spectral shape, the situation is more complex, but a linear combination can still be found that removes the background or at least most of it. The accuracy of the background removal will depend on the characteristics of the variation in the measurements. We attempt to explain this using two simple examples illustrated in Figure 13. Each example assumes we have 4 measurements, taken at different positions along the vehicle, denoted by spectra $M_A$, $M_B$, $M_C$, and $M_D$, and that the target and background spectral shapes change with the profile amplitudes as shown. The target and background spectral shapes are denoted by $\psi_i^T$ and $\psi_i^B$ respectively, where $i$ indicates the measurement location, that is, $A, B, C,$ or $D$. In the case on the right of Figure 13, based on the above assumptions, we have $\psi_A^B = \psi_B^B$ and $\psi_C^B = \psi_D^B$. Thus the linear combination $(M_B - M_A) + (M_C - M_D)$ removes the background and isolates the target with a large signal resulting from $(M_B + M_C)$. In the case on the left of Figure 13, using the same assumptions, the best nonsingular linear combination for isolating the target is given by $(\alpha_B M_B - \alpha_A M_A) + (\alpha_C M_C - \alpha_D M_D)$, where the coefficients are chosen to best remove the background. In this case there will be a residual background spectrum

that will be mixed with the target and will be reflected in the resulting TPCA fit to the target spectrum. It is important to note that these are idealized simple examples for illustration purposes only. For real problems the TPCA method will automatically chose the optimum coefficients for removal of the background for the chosen target model which needs to correctly represent the target in the measurements. The larger the number of measurements and the more limited the variation of the background spectral shape in the target region, the more likely it is for the TPCA method to accurately remove the background. Also, repeating and non-monotonic variation of the background spectral shape, not directly correlated with the target variation, are likely to result in better background removal while leaving a significant fraction of the target signal for analysis.

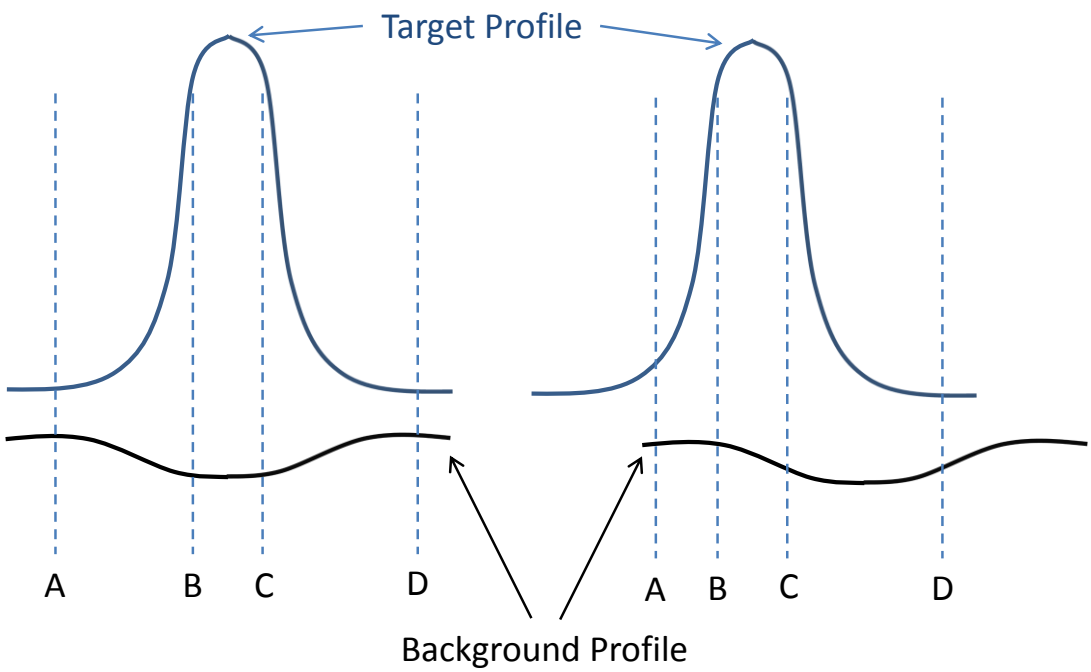


**Figure 13**. Illustrations of two sets of measurements for two cases with different target and background profiles. The measurement points are denoted by the vertical dashed lines.

## Representation of the Target Spectrum

Assuming that a proper linear combination is found to remove the background, this linear combination will result in a target spectrum that is a linear superposition of multiple spectra for the target at different shielding configurations. It is desirable that the overall target spectrum be represented by one spectrum at a set of effective shielding parameters. This is expected to be a good approximation when the shielding parameters do not vary significantly over the region that contributes the most target signal. Such is the case when the target signal extends over a narrow spatial region. In fact, for most gamma spectral analysis software programs, once a spatial region of interest (ROI) is found, the total spectrum in the ROI is analyzed for isotopic content using one set of effective shielding parameters that result in the optimum fit based on an optimization metric such as the $\chi^2$ residual.

To understand and quantify the limits of this approximation we consider a few simple tests where one spectrum is used to approximate a linear combination of two spectra for one target radionuclide at different shielding parameters. In other words, we seek to find the effective shielding parameters $AN_{Eff}$ and $AD_{Eff}$ that result in a best approximation for:

$$\gamma\, \psi_t(E, AN_{Eff}, AD_{Eff}) \approx \alpha\, \psi_t(E, AN, AD_1) + \beta\, \psi_t(E, AN, AD_2) \tag{12}$$

where all the quantities on the right hand side are specified. For the results shown below, the two spectra $\psi_t(E, AN, AD_1)$ and $\psi_t(E, AN, AD_2)$ are normalized to the same total counts so that contributions to the total spectrum are adjustable by the coefficients $\alpha$ and $\beta$. Figures 14-15 show results of fits to find the $AN_{Eff}$ and $AD_{Eff}$ for a combination of two spectra with different shielding parameters.

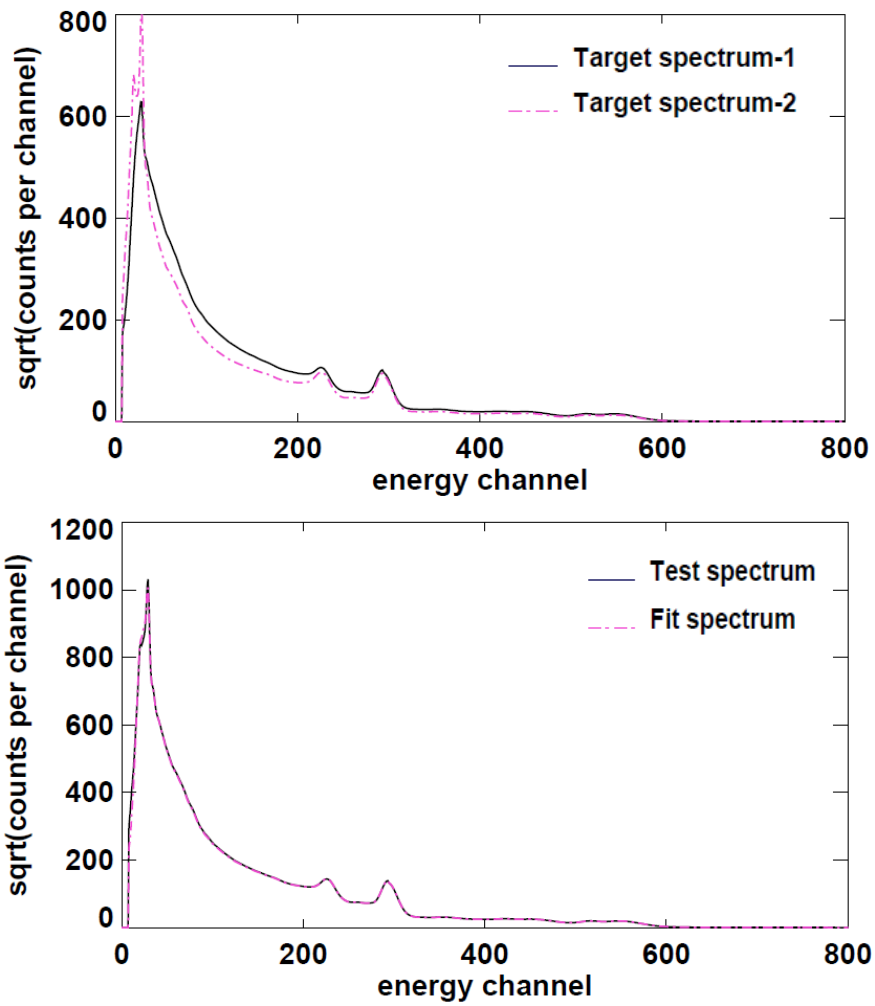


**Figure 14**. Top: test spectra at shielding parameters AN = 14.8, $AD_1$ = 25.0 and $AD_2$ = 10.0. The two spectra are normalized to the same total counts. Bottom: Test spectrum and fit at effective shielding parameters. The linear combination coefficients are: $\alpha = 1.0$ and $\beta = 1.0$. The best fit is obtained at AN = 14.0 and AD = 17.62.

These results show that, for the chosen examples, the fit to one target spectrum at an effective atomic number and areal density is accurate when the shielding parameters for the constituent spectra are not too disparate. Based on additional study similar to the results shown, it is expected that the approximation of a uniform areal density and atomic number for the target shielding is adequate for the embedded source problem. This is also expected based on the success of popular gamma spectral analysis software tools. It should be noted however, as observed in the example in Figure 15, that it is possible for the resulting effective atomic number to be significantly different from the true value when the combined spectra have disparate areal densities.

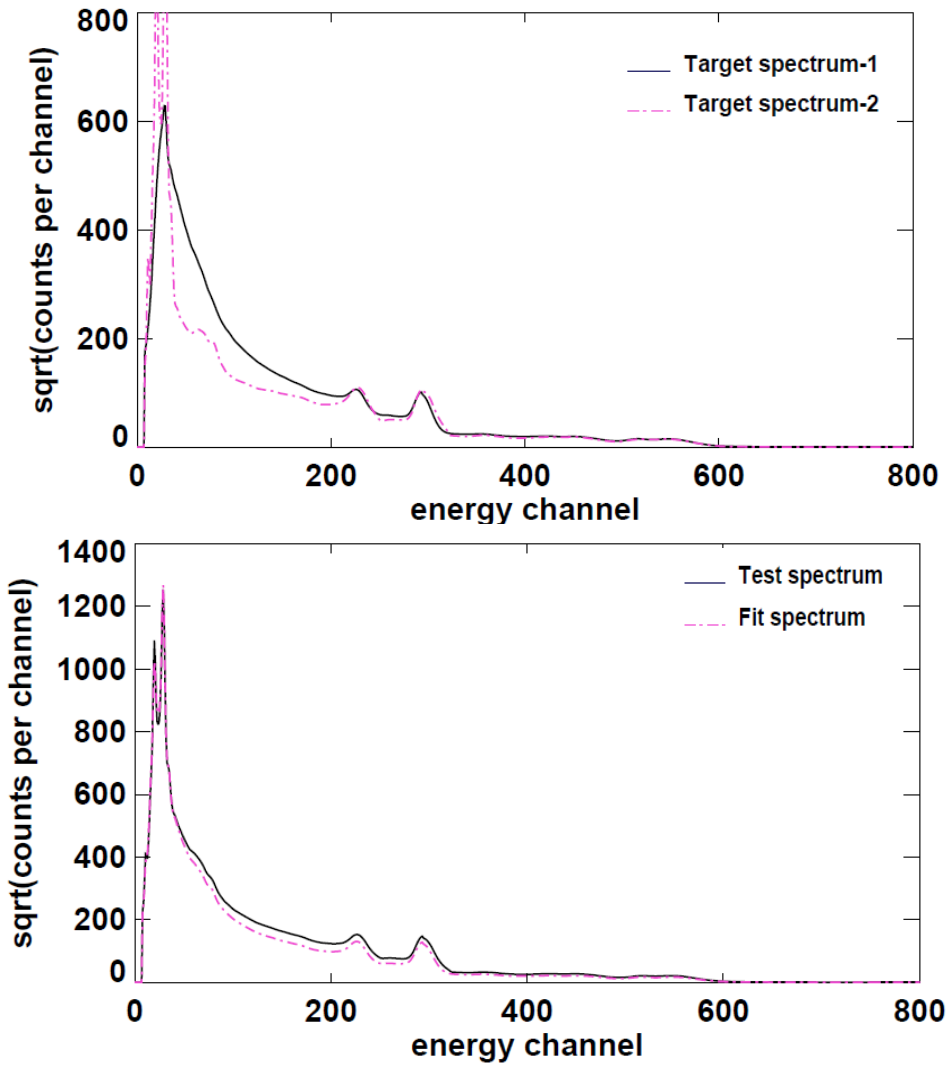


**Figure 15**. Top: test spectra at shielding parameters AN = 14.8, $AD_1$ = 25.0 and $AD_2$ = 2.0. The two spectra are normalized to the same total counts. Bottom: Test spectrum and fit at effective shielding parameters. The linear combination coefficients are: $\alpha = 1.0$ and $\beta = 1.0$. The best fit is obtained at AN = 17.33 and AD = 4.78.

# 6. Summary and Conclusions

In this report we have considered application of the TPCA method for detection of a shielded localized source that is embedded in a distributed source in a uniform background. This report complements a previous report (see reference 4) where the TPCA method was described in some detail and applied to detection of unshielded sources. This method uses spatial/temporal variations in multiple measurements to test the hypothesis of the presence of a target radionuclide of interest without having to identify other clutter radionuclides that are present. An essential requirement for the method to work properly is that the spatial distribution for the target of interest is different from that for the other clutter sources. Larger differences in the profiles are expected to improve detection limits.

When shielding effects are included, the target spectra depend on the atomic number and areal density of the shielding material in a nonlinear way. We used a simple interpolation method along with a library of shielded spectra to be able to estimate a shielded target spectrum for any set of shielding parameters. Currently the library has only three isotopes ($^{137}$Cs, $^{235}$U, and $^{238}$U) for a GR-135 detector. The library spectra were obtained using GADRAS. For the TPCA solution, the shielding parameters are estimated using a nonlinear optimization algorithm. This algorithm uses a coarse grid for evaluation of the minimizing function to localize the minimum followed by application of Powell's method using the Numerical Recipes function POWELL.

Within the limits of the assumptions made for generation of the simulation spectra, the results shown in this report verify that the TPCA method works well for shielded sources. The main assumption made is that all sources have constant spectral shapes for simulated measurements, that is, only the amplitude varies with spatial location. The effect of variation of target and background spectral shapes was briefly considered in the previous section. Variation of the target spectral shape for embedded localized sources, due to variable shielding, can be accounted for by the parametric target model used and is not expected to have a negative impact on results. The impact of variation of the background spectral shape will depend on the spatial distribution of this variation relative to the target distribution and can result in some error. Further study is needed to better quantify the effect of this variation.

In addition to effects of spectral shape variation, significant work is needed to understand optimization of method parameters, noise isolation in relation to the derived principal component spectra, and applicable constraints to limit residuals to physically realizable spectra. In addition, further work is required for estimation of target activity, localization, and estimation of detection limits and false positive rates.

## References


(1) Ely, J., Kouzes, R., Schweppe, J., Siciliano, E., Strachan, D., Weier, D.,"The Use of Energy Windowing to Discriminate SNM from NORM in Radiation Portal Monitors," Pacific Northwest National Laboratory SA 44680, *Nuclear Instruments and Methods in Physics Research A*, 560: 373-387, 2006.

(2) Burr, T., Gattiker, J. R., Myers, K. Tompkins, G. "Alarm criteria in radiation portal monitoring" *Applied Radiat. Isotopes* (2007)

(3) I. R. Shokair and D. Cohen, "Detecting Embedded Localized Radiation Sources by Using Radiation Portal Monitor Data", Sandia National Laboratories report SAND2008-3469, October 2008.

(4) I. R. Shokair, "Detection of Embedded Radiation Sources Using Temporal Variation of Gamma Spectral Data", Sandia National Laboratories report SAND2011-6453, September 2011.

(5) D. J. Mitchell, H. M. Sanger, and K. W. Marlow, "Gamma-Ray Response Functions for Scintillation and Semiconductor Detectors", *J. Nuc. Inst. And Methods in Physics Research A276* (1989), 547-556.

(6) D. R. Waymire and D. J. Mitchell, "GADRASw User Manual", updated November 2009.

(7) W. H. Press, S. A. Teukolsky, W. T. Vetterling, and B. P. Flannery, Numerical Recipes in C, Cambridge University Press, 1992.

(8) GEANT4 simulation toolkit: *Nuclear Instruments and Methods in Physics Research A 506 (2003) 250-303*, and *IEEE Transactions on Nuclear Science* 53 No. 1 .

# Distribution

1 Department of Homeland Security
Domestic Nuclear Detection Office
Attn: Brian Savage (electronic)

1 Department of Homeland Security
Domestic Nuclear Detection Office
Attn: Guy Hartsough (electronic)

1 Department of Homeland Security
Domestic Nuclear Detection Office
Attn: John Blackadar (electronic)

1 Department of Homeland Security
Domestic Nuclear Detection Office
Attn: David Chu (electronic)

1 Department of Homeland Security
Domestic Nuclear Detection Office
Attn: Greg Slovik (electronic)

1 Department of Homeland Security
Domestic Nuclear Detection Office
Attn: Luc Murphy (electronic)

1 Department of Homeland Security
Domestic Nuclear Detection Office
Attn: Jay Spingarn (electronic)

1 Lawrence Livermore National Laboratory
Attn: Simon Labov (electronic)

1 Los Alamos National Laboratory
Attn: Thomas L. Burr (electronic)

1 Los Alamos National Laboratory
Attn: Paul Felsher (electronic)

1 Pacific Northwest National Laboratory
Attn: Robert Runkle (electronic)

1 Pacific Northwest National Laboratory
Attn: Mark Tardiff (electronic)

1 Pacific Northwest National Laboratory
Attn: James Ely (electronic)

1 Pacific Northwest National Laboratory
Attn: David Pfund (electronic)

1 ManTech SRS Technologies, Inc.
Attn: Bruce Geelhood (electronic)

| | | | | |
|---|---|---|---|---|
| 1 | MS 0782 | Dean J. Mitchell | 6633 | (electronic copy) |
| 1 | MS 0782 | George Lasche | 6633 | (electronic copy) |
| 1 | MS 9004 | Peter B. Davies | 8100 | (electronic copy) |
| 1 | MS 9004 | Howard H. Hirano | 8110 | (electronic copy) |
| 1 | MS 9004 | Duane L. Lindner | 8120 | (electronic copy) |
| 1 | MS 9004 | James C. Lund | 8130 | (electronic copy) |
| 1 | MS 9003 | Jason C. Reinhardt | 8111 | (electronic copy) |
| 1 | MS 9003 | Alexander Roesler | 8112 | (electronic copy) |
| 1 | MS 9003 | Maynard Holliday | 8112 | (electronic copy) |
| 1 | MS 9003 | Gary W. Richter | 8112 | (electronic copy) |
| 1 | MS 9003 | Mathew Sumner | 8112 | (electronic copy) |
| 1 | MS 9056 | Thomas A. Reichardt | 8128 | (electronic copy) |
| 1 | MS 9104 | Willard R. Bolton | 8123 | (electronic copy) |
| 1 | MS 9104 | Troy E. Delano | 8123 | (electronic copy) |
| 5 | MS 9104 | Isaac R. Shokair | 8123 | |
| 1 | MS 9104 | Tim P. Tooman | 8123 | (electronic copy) |
| 1 | MS 9154 | William P. Ballard | 8200 | (electronic copy) |
| 1 | MS 9159 | Noel M. Nachtigal | 8958 | (electronic copy) |
| 1 | MS 9403 | Alfredo M. Morales | 8131 | (electronic copy) |
| 1 | MS 9402 | John E. M. Goldsmith | 8131 | (electronic copy) |
| 1 | MS 9402 | Arlyn J. Antolak | 8131 | (electronic copy) |
| 1 | MS 9402 | Kristin L. Hertz | 8131 | (electronic copy) |
| 1 | MS 9402 | Nathan R. Hilton | 8131 | (electronic copy) |
| 1 | MS 9402 | William C. Johnson | 8131 | (electronic copy) |
| 1 | MS 9402 | Christopher L. Kunz | 8131 | (electronic copy) |
| 1 | MS 9406 | Craig R. Tewell | 8132 | (electronic copy) |
| 1 | MS 9406 | Erik Brubaker | 8132 | (electronic copy) |
| 1 | MS 9406 | Scott Kiff | 8132 | (electronic copy) |
| 1 | MS 9406 | Peter Marleau | 8132 | (electronic copy) |
| 1 | MS 9406 | Wondwosen Mengesha | 8132 | (electronic copy) |
| 1 | MS0899 | RIM-Reports Management | 9532 | (electronic copy) |

Sandia National Laboratories